Rakenteiden Mekaniikka (Journal of Structural Mechanics)
Vol. 44, No 3, 2011, pp. 206-217

Virtual testing of cold-formed structural members

Petr Hradil, Ludovic Fülöp and Asko Talja

Summary. This paper introduces new modelling and evaluation algorithms for automated virtual testing of cold-formed structural members. These algorithms are integrated in Abaqus CAE plugin and verified against real tests of stainless steel hollow sections. Our tool is capable of creating finite element models including complex material behaviour, residual stresses and strains, enhanced material properties and geometrical imperfections. Also, it automatically evaluates the load carrying capacity of such models and creates test reports. The algorithms presented here can successfully assist engineers and researchers during the numerical analysis.

Key words: virtual testing, Abaqus, cold-formed steel, thin-walled structures, stainless

Introduction

In civil engineering structures, the use of thin walled cold-formed profiles has many advantages that result in their growing popularity. However, proper design of such elements is more demanding because of local stability issues in their load carrying capacity predictions. Typically, time consuming and expensive experimental tests are carried out in order to exploit the advantages of good weight to capacity ratio. These tests can be technically difficult and often influenced by many uncertainties. In case of steel structures, there is always possibility to create a finite element model which would be able to simulate the experiment with good accuracy, but performing such analysis requires advanced software, expert user skills and a plenty of time. Considerably long time is spent on creating a model that has to be three-dimensional, preferably composed by shell elements and sometimes perturbed by geometrical imperfections. Moreover, the difficulty of this modelling increases when the need of nonlinear material behaviour, enhanced corner properties and residual stresses has to be satisfied.

Although the development of computational software for civil engineering has advanced rapidly in recent years, the steel structures computational models are still mostly represented as beam elements that are insufficient for evaluating cold-formed profiles. Our goal was to address the gap between these programs and universal multiphysic simulation tools (e.g. Ansys or Abaqus) by creating an algorithm that automates most of the laborious tasks during finite element modelling. Therefore, we developed a plugin for Abaqus CAE that simulates laboratory experiments on thin walled structural members; especially those made of carbon and stainless steel. This tool can provide additional data to real experiments or even replace them. The presented tool can also serve as a basis for more accurate design of cold-formed steel structures and have a potential of replacing the traditional models composed of beam elements.

Geometry and experimental setups

The virtual testing tool presented in this paper is primarily focused on cold-formed steel members, and therefore all the geometry is exclusively modelled using shell elements. The selection of all standard Abaqus shell elements is extended by S9R5 nine-node element with reduced integration, which is otherwise not available in CAE, but has a good performance in the nonlinear analyses of cold-formed steel structures [1]. The internal meshing algorithm included in the script is giving a full control of each node position to the program. A user usually selects only the maximum node spacing and the number of segments forming rounded corners.

The shape of member cross-section defines most of the geometry and is therefore an important part of the user interface. Each cross-section shape is parametrically defined in our tool, and can produce infinite number of members of the same type. The possibility to use a library of pre-defined cross-sections decreases the whole modelling time into few seconds; requiring only basic dimensions to be entered. Even inserting a new cold-formed shape into the library is easier than creating the whole model from scratch (Figure 1).

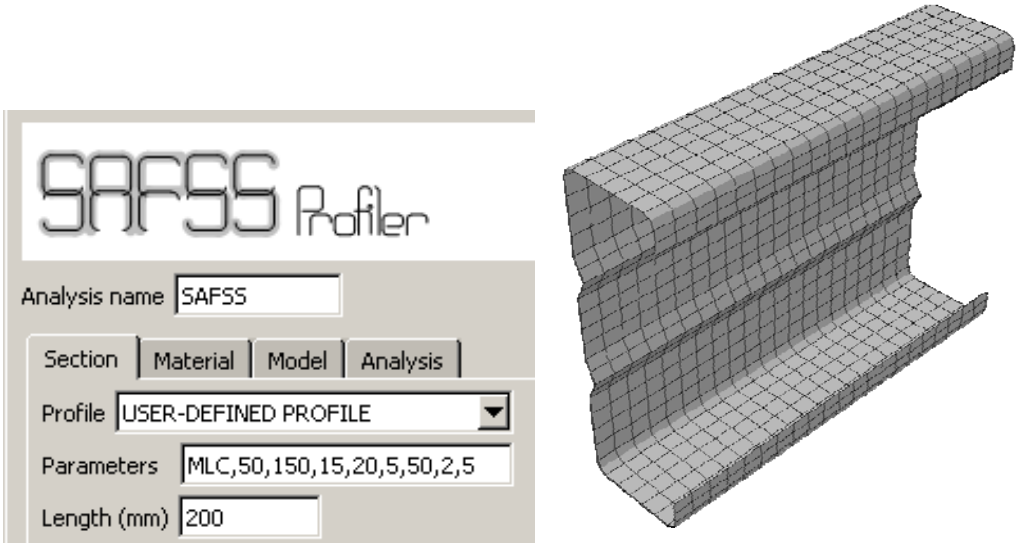

Figure 1. The possibility to create complex user-defined cross-sections.

The virtual testing tool contains a library of predefined experimental set-ups that can be easily modified by the user as illustrated in Figure 2. The type and position of supports, loads and measuring points can be entered in the configuration file, which enables a large variety of experiments ranging from simple tension, compression or stub-column tests to more complex bending or web-crippling experiments. It is also possible to change loads into displacements and simulate displacement-controlled tests.

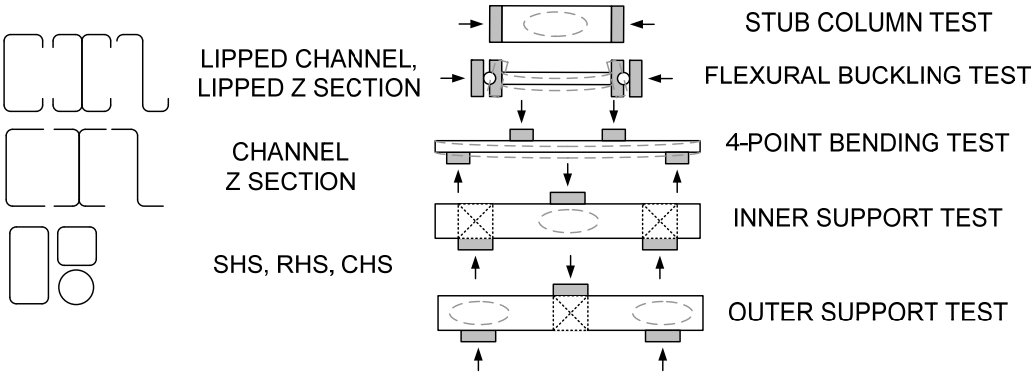

Figure 2. Examples of basic library elements.

Material models and initial conditions

The selection of material models in virtual testing tool ranges from the most simple elastic-plastic behaviour up to complex nonlinear materials (e.g. high strength steel, aluminium and stainless steel). The most advanced nonlinear material models can be taken as Ramberg & Osgood's [2], Mirambel & Real's [3], Rasmussen's [4] or Gardner's [5] model. The stresses and strains are calculated as engineering values and then converted into true stresses and logarithmic plastic strains.

Ramberg & Osgood model with Hill's modification

The basic nonlinear material model was originally developed for aluminium alloys, but was proved to be suitable also for other metallic materials [2]. The stress and strain relation is defined by the initial modulus of elasticity E_0, 0.2% proof stress $\sigma_{0.2}$ and the nonlinear factor n.

$$\varepsilon = \frac{\sigma}{E_0} + 0{,}002\left(\frac{\sigma}{\sigma_{0.2}}\right)^n \tag{1}$$

This model is included in AS/NZS 4373:2001 [6], Eurocode 3, Part 1-4 [7] (calculation of deflections) and SEI/ASCE [8].

Mirambell & Real model

This model developed from Ramberg & Osgood formula is able to describe the material behaviour more precisely for plastic strains larger than 0.2% [3]. It introduces a new Ramberg & Osgood curve originating from 0.2% proof stress as described in equation (2), where the initial tangent modulus $E_{0.2}$ is defined by the slope of the previous stage in equation (3) and the parameter of non-linearity is called m. The second stage then continues to the ultimate stress and strain σ_u and ε_u respectively.

$$\varepsilon = \frac{\sigma - \sigma_{0.2}}{E_{0.2}} + \varepsilon^* \left(\frac{\sigma - \sigma_{0.2}}{\sigma_u - \sigma_{0.2}} \right)^m + \varepsilon_{0.2} \text{ when } \sigma > \sigma_{0.2}$$
$$\text{where } \varepsilon^* = \varepsilon_u - \varepsilon_{0.2} - \frac{\sigma_u - \sigma_{0.2}}{E_{0.2}}, \tag{2}$$

The 0.2% strain and tangent modulus can be calculated as:

$$\varepsilon_{0.2} = \frac{\sigma_{0.2}}{E_0} + 0.002 \text{ and } E_{0.2} = \frac{E_0}{1 + 0.002n\left(E_0 / \sigma_{0.2}\right)} \tag{3}$$

Rasmussen's model

Rasmussen's study reduces the six parameters of Mirambell & Real model to three by proposing the calculation of the second nonlinear parameter *m*, ultimate stress and ultimate strain [4]. It is based on experiments carried out on stainless steels, mainly austenitic and duplex grades. Rasmussen's model is included in informative Annex C of Eurocode 3, Part 1-4 [7].

Gardner's model

Gardner proposes another modification of Mirambell & Real's material model, where the second part of Ramberg & Osgood's curve passes through, 1.0% proof stress $\sigma_{1.0}$ instead of ultimate stress [5] as seen in equation (4). This approach is supposed to be more convenient because it can include also compressive behaviour.

$$\varepsilon = \frac{\sigma - \sigma_{0.2}}{E_{0.2}} + \varepsilon^* \left(\frac{\sigma - \sigma_{0.2}}{\sigma_{1.0} - \sigma_{0.2}} \right)^{n_{0.2,1.0}} + \varepsilon_{0.2} \text{ when } \sigma > \sigma_{0.2},$$
$$\text{where } \varepsilon^* = \varepsilon_{1.0} - \varepsilon_{0.2} - \frac{\sigma_{1.0} - \sigma_{0.2}}{E_{0.2}} \tag{4}$$

Enhanced material properties

The enhanced material properties in the virtual testing tool can be calculated separately in the flat parts (f) and corners (c) using virgin material values (v). Three different methods for calculating enhanced material properties can be used as presented in Table 1 and Figure 3.

The method proposed by Cruise and Gardner [9] is based on the experiments of press-braked and cold-rolled stainless steel sections and the calculation in Rossi et al. [10] originates from the analytical inversion of material model published by Abdella [11]. The ultimate stress is calculated using a method proposed by Ashraf et al. [12]. If no predictive method is selected in the tool, the material strength is treated as the average property of the whole cross-section as defined in Eurocode 3, Part 1-3.

Table 1. Enhanced material properties.

Stress	Method A	Method B	Method C
	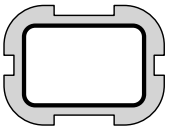		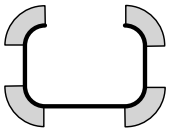
	Cold-rolled (corner extension *2t*)		Press-Braked
$\sigma_{02,f}$	Cruise, 2008	Rossi, 2010	(no change)
$\sigma_{u,f}$	Cruise, 2008	Cruise, 2008	(no change)
$\sigma_{02,c}$	Cruise, 2008	Rossi, 2010	Cruise, 2008
$\sigma_{u,c}$	Ashraf et al., 2005	Ashraf et al., 2005	Ashraf et al., 2005

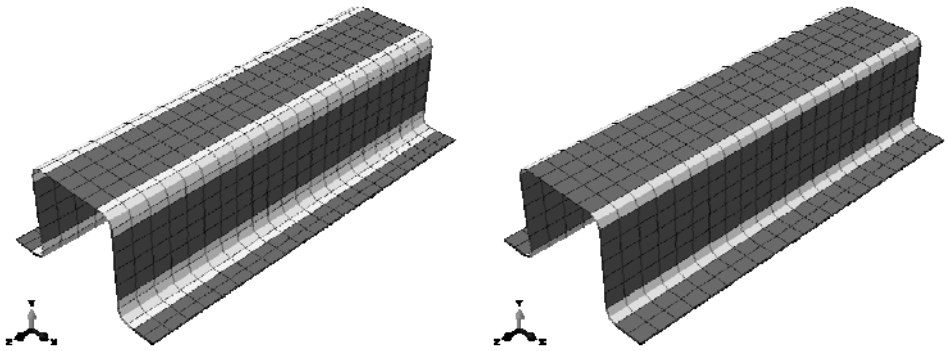

Figure 3. Material property distribution for cold-rolled (left) and press-braked profiles (right).

Residual stresses

For the magnitude of bending residual stresses surface values, the Gardner and Cruise's approach is used [13], which was tested on stainless steel hollow sections made by circle-to-rectangle forming process and press-braked sections (Figure 4). The residual stresses are inserted as initial model conditions using Abaqus keyword *INITIAL CONDITIONS with a through-thickness fully plastic distribution. The corresponding residual strains are inserted with a through-thickness linear distribution.

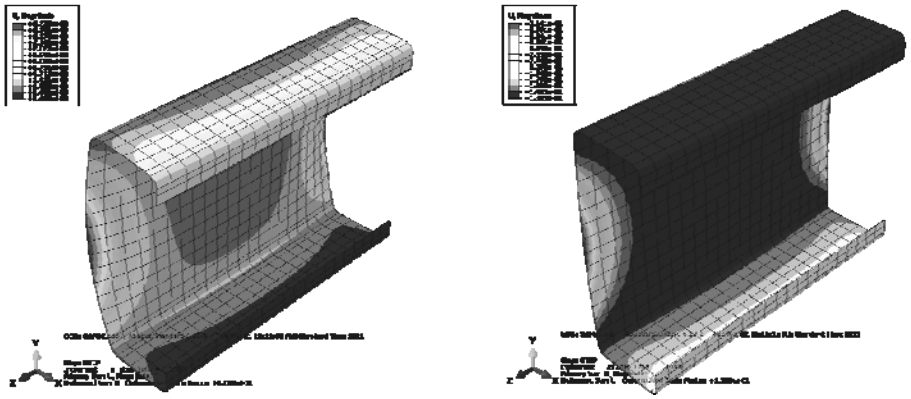

Figure 4. Cold-rolled C section (left) and press-braked C (right) – deformation after stress release (10x scaled).

Numerical analysis

The virtual testing tool analysis is based on the arc-length (Riks) method that gradually increases the loads or displacements until the conditions selected by user are met. The termination criterion is usually chosen so that the analysis ends when the load starts to decrease, which is not standard termination condition in Abaqus, and therefore a monitoring method had to be developed to save computational time.

Initial imperfections

The stability failure is expected in many experiments involving thin-walled steel elements. In such cases, the calculation requires also initial imperfection distribution in order to carry out proper geometrically and materially nonlinear analysis on imperfect structure (GMNIA). In addition, the combination of more buckling modes can be required. The virtual testing tool offers a possibility to combine initial imperfections from several different sources and is able to automatically perform linear eigenvalue analysis (LEA) prior to the GMNIA calculation in order to obtain imperfection distribution. It also contains the algorithm for constrained LEA that produces only overall buckling modes [14] for easy separation of local and global imperfections (Figure 5).

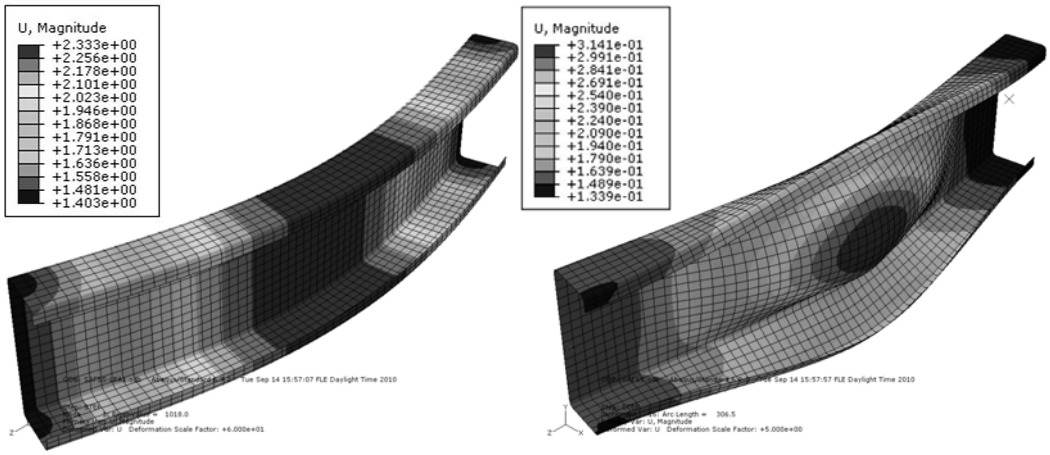

Figure 5. Constrained LEA analysis (left) and the final deformed shape in GMNIA (right).

Finally, the tool writes a test report. It is automatically generated in HTML including measured data, recorded maximum load, and figures of buckling modes and a final shape of deformed specimen from GMNIA analysis.

Verification

The virtual testing tool was checked against many physical experiments, but only four representative tests are presented here. Bending and tensile tests of ferritic stainless-steel hollow sections were performed in VTT by Talja et al. [15], where SHS 80x80x2 and RHS 40x80x2 profiles from grade 1.4009 stainless steel were supplied by

Table 2. Geometry of test specimen.

Test type	Specimen	Member width b (mm)	Member height h (mm)	Steel thickness t (mm)	Corner radius r (mm)	Member length L (mm)
Bending	RHS_BE	79.97	40.11	1.96	4.63	1000
	SHS_BE	79.63	79.90	1.97	3.81	999
Tension	RHS_MA0	79.98	40.01	1.98	4.56	2000
	SHS_MA0	80.08	80.03	1.96	4.00	2000

Table 3. Material properties of test specimen (hollow sections) used in FE analysis.

	E_0 (MPa)	σ_{02} (MPa)	n	σ_u (MPa)	m	ε_u
Average material RHS	190710	520	5.7	557	1.64	0.0097
Average material SHS	195592	502	6.1	527	4.07	0.0123
Virgin material	168546	346	12.1	481	1.00	0.0041

Table 4. Enhanced material properties in full-member test simulations.

Enhanced material properties		0.2% proof stress			Ultimate strength		
		$\sigma_{0.2,v}$ (MPa)	$\sigma_{0.2,f}$ (MPa)	$\sigma_{0.2,c}$ (MPa)	$\sigma_{u,v}$ (MPa)	$\sigma_{u,f}$ (MPa)	$\sigma_{u,c}$ (MPa)
RHS	From tensile tests	346	520		481	557	
	Method A [1)]	346	432	434	481	523	523
	Method B [1)]	346	546	553	481	553	553
SHS	From tensile tests	346	502		481	527	
	Method A [1)]	346	401	427	481	515	515
	Method B [1)]	346	511	543	481	543	543

1) Predictive methods are described in Table 1

Stalatube Oy. The geometry of specimens was measured in several points and the average values for each member were used in finite element calculations (Table 2).

The material model used in finite element simulations was based on the Mirambell-Real two-stage calculation and its parameters were optimized to match the stress and strain measurement of real material. Coupons for the material tests were cut from the original metal sheet and average material properties were calculated from the load-displacement relationship of the whole member tension test. The optimization results are presented in Table 3.

Two analytical models for prediction of strength enhancement in cold-rolled stainless steel sections were used and compared to the data measured on coupons from the cold-formed sections in Table 4. The finite element models also contained bending residual stresses and strains distributed according to Jandera et al. [16].

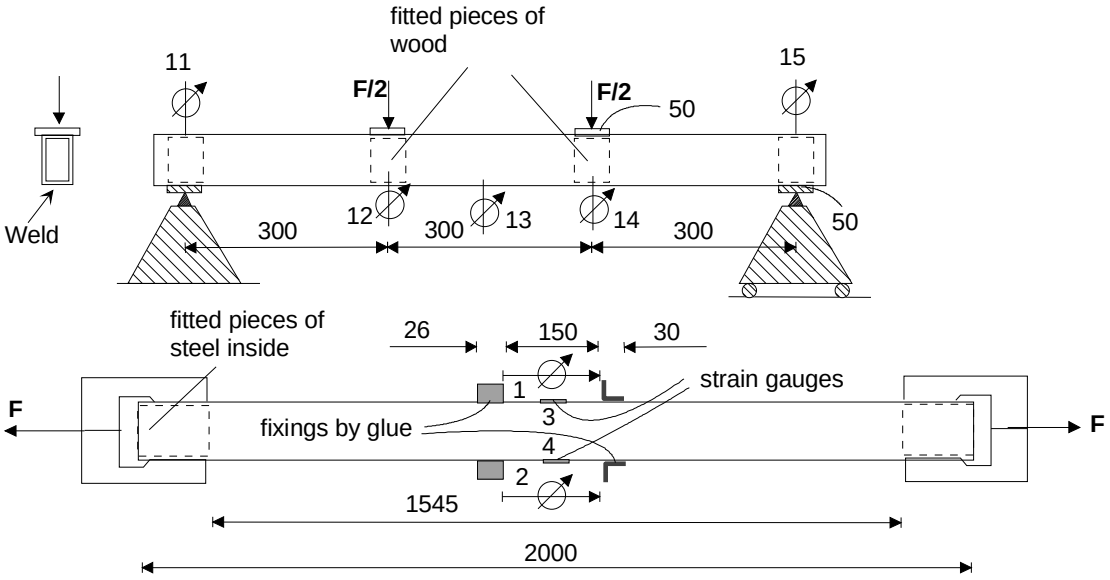

Figure 6 Experiment set-up for bending tests (top) and tensile tests (down).

Numerical models were composed of S4R shell elements with reduced integration and five section points. The maximum node spacing was 5 mm and corners were modelled with three segments. The test setups were predefined according to designs in Figure 6 while the total member lengths and cross-sectional dimensions were always adjusted to the measured values from Table 2. Initial imperfections were distributed according to LEA analysis and scaled to values recommended by Eurocode.

In case of bending tests, simplifications of the real geometry in the loading and support areas were made in order to simulate the experiment with acceptable accuracy and to keep numerical model simple without contacts (Figure 7). The load was applied on model lines in longitudinal direction and supports were modelled as rigid faces with boundary conditions in their centre of gravity. This allows appropriate displacement and rotation. Because of the local buckling of compressed face was expected to be the ultimate failure, the initial imperfections from the first local buckling mode were scaled to the amplitude of $b/200$. No eigenvalue analysis was needed for the tensile test simulation.

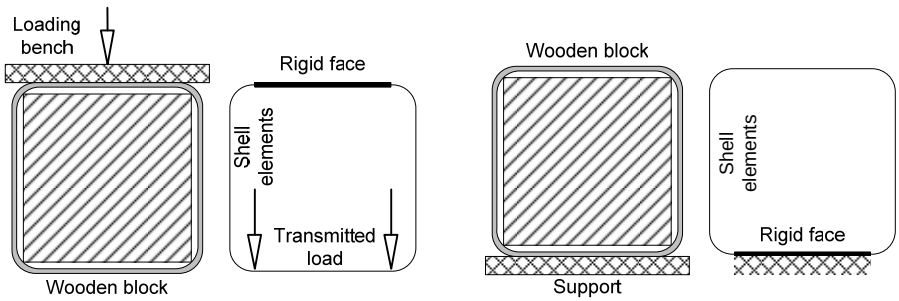

Figure 7. Real configuration and model simplification under the load (left) and at the support (right) in bending tests.

Table 5. Load-carrying capacity of tested specimen and FEM calculations.

Test type	Specimen	Predicted capacity (kN)				Real capacity (kN)
		R_{TT}	R_{MA}	R_{MB}	R_{EC}	R_{EXP}
Bending	RHS_BE	39.3	34.0	38.9	33.9	39.7
	SHS_BE	47.0	40.7	46.9	40.6	54.0
Tension	RHS_MA0	255	239	252	256	245
	SHS_MA0	323	314	330	323	320

Table 6. Ratios of experimental and predicted load carrying capacity.

Test type	Specimen	Capacity ratio			
		R_{EXP}/R_{TT}	R_{EXP}/R_{MA}	R_{EXP}/R_{MB}	R_{EXP}/R_{EC}
Bending	RHS_BE	1.00	1.16	1.00	1.17
	SHS_BE	1.13	1.33	1.13	1.33
Tension	RHS_MA0	0.96	1.03	0.97	0.96
	SHS_MA0	0.99	1.02	0.97	0.99

Several models of material distribution were applied in finite element calculations (R_{TT} – material from tensile tests of coupons, R_{MA} – Method A, R_{MB} – Method B, described in Table 4). The load carrying capacity of tested specimen was also calculated using the analytical formulas from Eurocode 3 [7] and effective cross-section in bending (R_{EC} in Table 5). Measured load-carrying capacity of the whole member in bending and tension was compared with the ultimate load calculated by GMNIA analysis in Table 6.

The results in Table 6, Figures 8 and 9 show that the finite element analysis is able to provide a good prediction of cold-formed elements load-displacement behaviour if their dimensions and material properties are provided. The accuracy of presented calculation can be further increased by measuring real imperfections amplitude and distribution.

Predicting a load carrying capacity of stainless steel cold-rolled hollow sections is particularly difficult because of the limited knowledge of changes in material parameters during work hardening and because of relatively high level of residual stresses that have to be accounted for. Two models for estimation of material strength enhancement were used and better agreement was observed in case of the model B (proposed by Rossi et al. [10]). This calculation was nearly as accurate as using the real material properties tested in work hardened conditions. The difference between SHS and RHS ratios in Table 6 could be caused by unequal strength in section faces. In fact, the shorter faces in rectangular section had 7% higher yield strength than the average value.

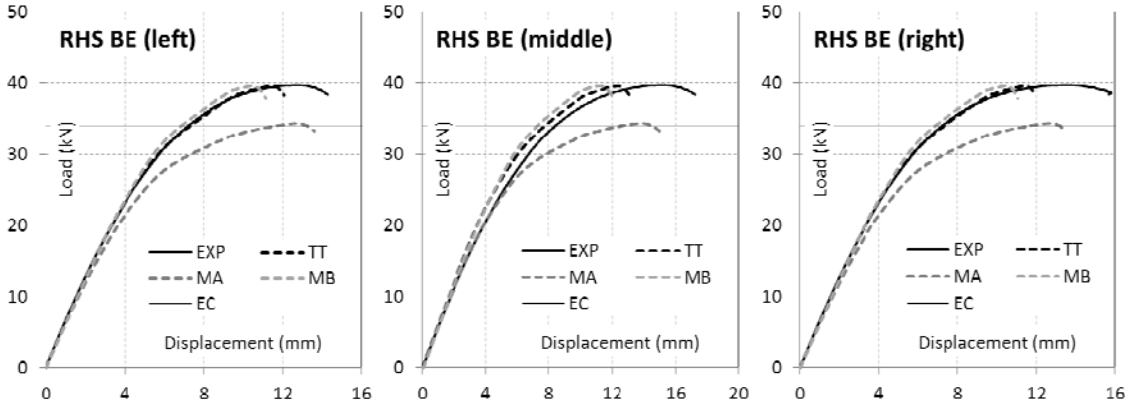

Figure 8. Comparison of numerical (Tensile test, Method A,B and Eurocode) and experimental (EXP) results in RHS section bending test; deflections were measured in three different points.

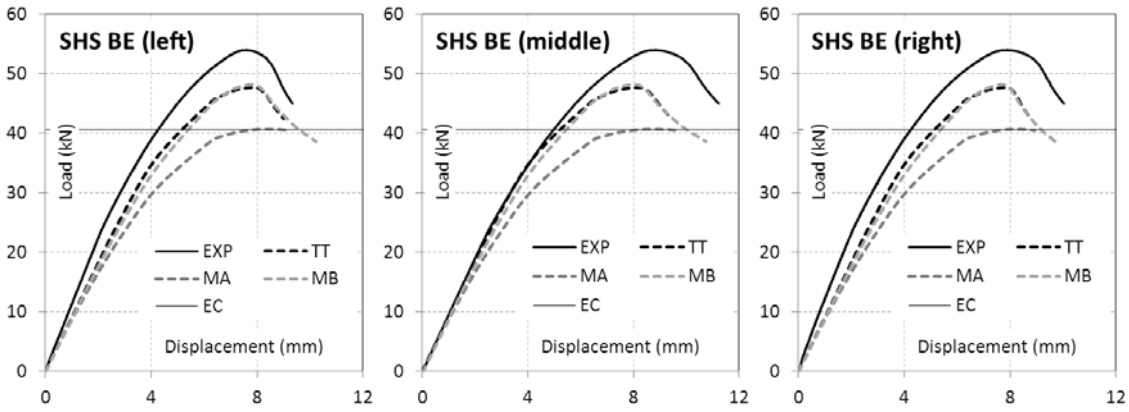

Figure 9. Comparison of numerical (Tensile test, Method A,B and Eurocode) and experimental (EXP) results in SHS section bending test; deflections were measured in three different points.

Conclusions

Although the calculations of cold-formed structural members require advanced numerical tools, only limited options of modelling each phenomenon are applicable in this particular area. Therefore a software capable of generating and evaluating numerical models of cold-formed elements can perform many tasks automatically, save the time and decrease the risk of errors caused by manual modelling. The possibility of carrying out series of calculations in predefined batches increases the efficiency of the analysis even more and enables performing complex task like shape optimization, parametric studies or strength curves prediction.

An example of such tool was presented in this paper. The accuracy of two different predictive models for enhanced material properties was tested using our software and results showed a good agreement with experimental tests.

Based on limited calibration like presented here, a small design office or cold-formed profile manufacturer can easily perform complex tasks (e.g. optimizing the shape and dimensions of their products, or develop design tables for an existing range of cold-formed products). Using the virtual testing tool they can undertake this with limited knowledge of finite element modelling and with substantially reduced effort.

Another potential application area of the tool is the support for testing labs. Quite often the results of a physical experiment leave unanswered questions related to the particular behaviour or failure observed. Before moving to the next experiment, the laboratory engineer can run a virtual experiment of and clarify the unclear effects in the physical test, by using the full capacity that numerical modelling offer. Then he can move to the next physical test with more confidence. Moreover, running the virtual experiment before the real one may provide important information about estimated specimen behaviour and the laboratory equipment can be adjusted accordingly. Using our tool, this can be done instantaneously and with no particular experience in finite element analysis.

Acknowledgements

The research leading to these results has received funding from the European Community's Research Fund for Coal and Steel (RFCS) under Grant Agreement No. RFSR-CT-2010-00026, Structural Applications of Ferritic Stainless Steels.

References

[1] B.W Schafer, T. Peköz, Computational modeling of cold-formed steel: characterizing geometric imperfections and residual stresses. *Journal of Constructional Steel Research* 47(3): 193-210, 1998.

[2] W. Ramberg, W.R. Osgood, *Description of stress-strain curves by three parameters,* Technical Note No. 902. USA: National Advisory Committee for Aeronautics, 1943.

[3] E. Mirambell, E. Real, On the calculation of deflections in structural stainless steel beams: an experimental and numerical investigation. *Journal of Constructional Steel Research*, 54(1):109-133, 2000.

[4] K.J.R. Rasmussen, Full-range stress–strain curves for stainless steel alloys. *Journal of Constructional Steel Research*, 59(1): 47-61, 2003.

[5] L. Gardner, M. Ashraf, Structural design for non-linear metallic materials. *Engineering Structures,* 28(6): 926-934, 2006.

[6] Standards Australia & Standards New Zealand, *Australian/New Zealand Standard: Cold-formed stainless steel structures.* Australia: 2001.

[7] European Committee for Standardization, *Eurocode 3: Design of steel structures, Part 1-4: General rules. Supplementary rules for stainless steels*. Belgium: 2006.

[8] ASCE/SEI, *Specification for the Design of Cold-Formed Stainless Steel Structural Members*. USA: 2002.
[9] R.B. Cruise, L. Gardner, Strength enhancements induced during cold forming of stainless steel sections. *Journal of Constructional Steel Research*, 64(11): 1310-1316, 2008.
[10] B. Rossi, H. Degée, F. Pascon, Enhanced mechanical properties after cold process of fabrication of non-linear metallic profiles. *Thin-Walled Structures*, 47(12): 1575-1589, 2009.
[11] K. Abdella, An explicit stress formulation for stainless steel applicable in tension and compression. *Journal of Constructional Steel Research*, 63(3): 326-331, 2007.
[12] M. Ashraf, L. Gardner, D.A. Nethercot, Strength enhancement of the corner regions of stainless steel cross-sections. *Journal of Constructional Steel Research*, 61(1): 37-52, 2005.
[13] L. Gardner, R.B. Cruise, Modeling of Residual Stresses in Structural Stainless Steel Sections. *Journal of Structural Engineering*, 135(1): 42-53, 2009.
[14] L. Zhang, G.S. Tong, Lateral buckling of web-tapered I-beams: A new theory. *Journal of Constructional Steel Research*, 64(12): 1379-1393, 2008.
[15] A. Talja, P. Hradil, SAFSS WP2, *Task 2.3: Model calibration tests, test report*, VTT, Finland, 2011.
[16] M. Jandera, L. Gardner, J. Macháček, Residual stresses in cold-rolled stainless steel hollow sections. *Journal of Constructional Steel Research*, 64(11): 1255-1263, 2008.

Petr Hradil, Ludovic Fülöp and Asko Talja
VTT, Technical Research Centre of Finland
Kemistintie 3, PL 1000 02044 VTT, Finland
petr.hradil@vtt.fi